Structural Engineering and Mechanics, *Vol. 73, No. 5 (2020) 487-500*
DOI: https://doi.org/10.12989/sem.2020.73.5.487

A comparison of structural performance enhancement of horizontally and vertically stiffened tubular steel wind turbine towers

Yu Hu[1,2a], Jian Yang*[1,2], Charalambos C. Baniotopoulos[2c] and Feiliang Wang[1d]

[1]School of Naval Architecture, Ocean and Civil Engineering, Shanghai Jiao Tong University, Shanghai 200240, China
[2]School of Civil Engineering, University of Birmingham, Edgbaston, Birmingham, B15 2TT, United Kingdom

(Received July 5, 2018, Revised August 12, 2019, Accepted October , 2019)

Abstract. Stiffeners can be utilised to enhance the strength of thin-walled wind turbine towers in engineering practise, thus, structural performance of wind turbine towers by means of different stiffening schemes should be compared to explore the optimal structural enhancement method. In this paper two alternative stiffening methods, employing horizontal or vertical stiffeners, for steel tubular wind turbine towers have been studied. In particular, two groups of three wind turbine towers of 50m, 150m and 250m in height, stiffened by horizontal rings and vertical strips respectively, were analysed by using FEM software of ABAQUS. For each height level tower, the mass of the stiffening rings is equal to that of vertical stiffeners each other. The maximum von Mises stresses and horizontal sways of these towers with vertical stiffeners is compared with the corresponding ring-stiffened towers. A linear buckling analysis is conducted to study the buckling modes and critical buckling loads of the three height levels of tower. The buckling modes and eigenvalues of the 50m, 150m and 250m vertically stiffened towers were also compared with those of the horizontally stiffened towers. The numbers and central angles of the vertical stiffeners are considered as design variables to study the effect of vertical stiffeners on the structural performance of wind turbine towers. Following an extensive parametric study, these strengthening techniques were compared with each other and it is obtained that the use of vertical stiffeners is a more efficient approach to enhance the stability and strength of intermediate and high towers than the use of horizontal rings.

Keywords: wind turbine tower; shell structures; stiffening rings; vertical stiffeners; parametric study; finite element analysis

1. Introduction

As stiffening rings are traditionally employed to strengthen cylindrical shells, horizontal ring stiffeners are nowadays used extensively in engineering practice to enhance the strength of thin-walled structures against buckling. In 1998, Chen and Rotter (1998) proposed an integrated approach to predict the membrane and bending stresses of asymmetric stiffening rings on cylindrical shells under axisymmetric loadings. Some years later, Lemak and Studnicka (2005) investigated the effect of the spacing and stiffness of stiffening rings on a steel cylindrical shell, and concluded with the proposal of a method for the determination of the maximum distance between neighbouring stiffeners. Qu *et al*. (2013) studied the dynamic characteristics of conical-cylindrical-spherical shells enhanced by stiffening rings, and a good agreement between experimental and FEM results was achieved in terms of natural frequencies and mode shapes. Showkati and Shahandeh (2010) investigated the process of the collapse of ring-stiffened pipelines under hydrostatic pressure, and also studied the effect of stiffening rings on the buckling behaviours of the pipelines. Gong *et al.* (2013) studied the effect of stiffening rings on the critical harmonic settlement of thin-walled tanks. Zhao *et al.* (2002) looked at the vibration of laminated circular cylindrical shells with orthogonal stiffeners by comparing numerical and experimental results. Sabouri-Ghomi *et al.* (2006) evaluated the effect of stiffening rings on the buckling behaviours of concrete cooling towers using numerical analysis. Lavassas *et al.* (2003) proposed the enhancement of the structural response of a 44m high tower with stiffening rings under gravity, seismic and wind loadings based on the relevant Eurocodes. Lupi *et al.* (2013) analysed a newly identified type of bistable flow around circular cross-section cylinders with stiffening rings through wind tunnel testing, and Ross *et al.* (2005) thoroughly investigated the plastic buckling of conical shells with stiffening rings under water pressure. Makarios *et al.* (2014) performed modal analysis by the continuous model method for a prototype of a 76m wind turbine tower. Baniotopoulos *et al.* (2011, 2007) systematically introduced the design of wind energy structures subjected to wind loadings. Nguyena *et al.* (2017) measured the vibration behaviors of hybrid bolt-loosening detection of wind turbine tower manufactured by rectangular hollow cross-sections with bolt-connections. Alonso-Martinez *et al.* (2019) simulated the flange area where the failure had occurred, including the bolts, their prestressing forces and the contact between the joined

*Corresponding author, Professor
E-mail: j.yang.1@sjtu.edu.cn
[a] Post Doctorate Researcher
E-mail: huyu1012@hotmail.com
[b] Professor
E-mail: C.Baniotopoulos@bham.ac.uk
[c] Post Doctorate Researcher
E-mail: wongfayeleung@163.com

http://www.techno-press.com/journals/sem&subpage=7
ISSN: 1225-4568 (Print), 1598-6217 (Online)

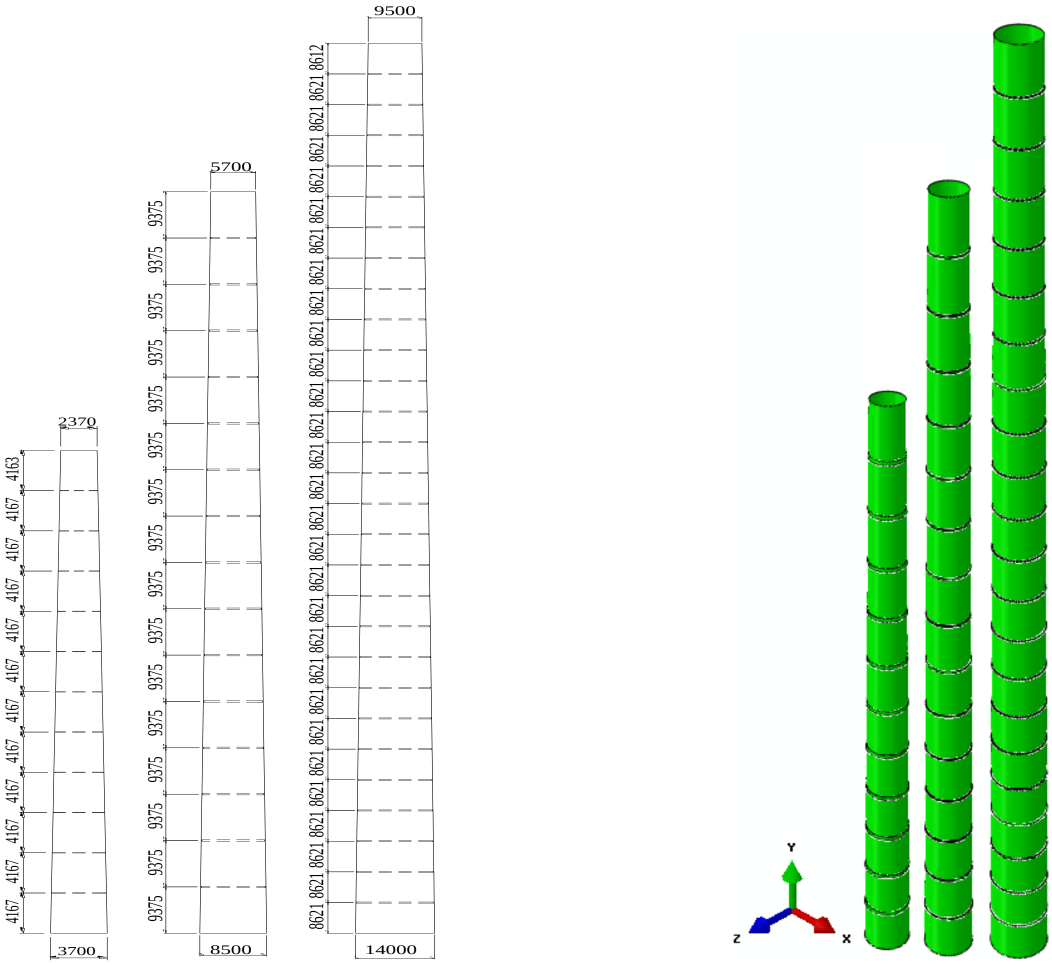

(a) Geometrical data of the prototypes (b) FEM models

Fig. 1 Prototypes of 50m, 150m and 250m ring-stiffened towers (in mm)

surfaces to explore the failure cause of wind turbine towers. Adhikaria and Bhattachary (2012) proposed a simplified method to study the free vibration of offshore wind turbine tower with flexible foundation.

Nowadays, wind turbines supported by high towers are extensively used to harvest wind energy due to their zero carbon dioxide emissions. These towers are often tubular steel structures with a relatively small wall thickness in relation to the diameter of the tower cross-section and height. Thus, these cylindrical tubular towers are considered to be typical slender structures. As all slender structures are vulnerable to local and overall buckling, stiffeners need to be added to the tower structure to enhance its structural response. Stiffeners are secondary sections used to strengthen the thin-walled structures against out-of-plane deformations. As previously mentioned, thin-walled towers are usually stiffened by stiffening rings. However, to improve the effect of the various stiffeners on the structural response of shell structures under wind loads, vertical stiffeners can be also added to the inside of towers. Hull (2012) proposed a three-dimensional analytical solution of a cylinder with vertical stiffeners and compared it with FEM results. Wójcik *et al.* (2011) assessed the linear and non-linear buckling behaviour of a cylindrical metal bin with vertical stiffeners under axisymmetric and non-axisymmetric loads, and the simulated buckling loads were compared with results based on existing guidelines. Xie and Sun (2009) investigated the vibration response of a cylindrical shell with vertical stiffeners excited by acoustic waves. Lee and Yoo (2012) evaluated the effect of longitudinal stiffeners on the stability of concrete-filled tubes. In 2007, Ramachandran and Narayanan (2007) predicted the modal density and radiation efficiency of a cylinder with vertical stiffeners, and verified the predicted results by comparing them with experimental results. Rotter and Sadowski (2012) solved the equations of shell bending theory for stiffened orthotropic cylindrical shells under axisymmetric pressure. Torkamani *et al.* (2009) conducted the free vibration of orthogonally stiffened cylindrical shells by using structural similitude theory. Bray and Egle (1970) carried out experiments on free vibrations of thin cylinrical shells stiffened with longitudinal stiffeners, and the experimental results were compared to theoretical results, and a close correlation between analytical and experimental results was found. Iwicki *et al.* (2011) studied the failure of cylindrical steel silos with vertical stiffeners by means of a linear and a non-linear buckling analysis taking into account geometric and material nonlinearities. Rebelo *et al.* (2012a, 2012b) experimentally monitored the structural response of an actual 76m wind turbine tower within 15 months measurement and analysed the dynamic responses of the

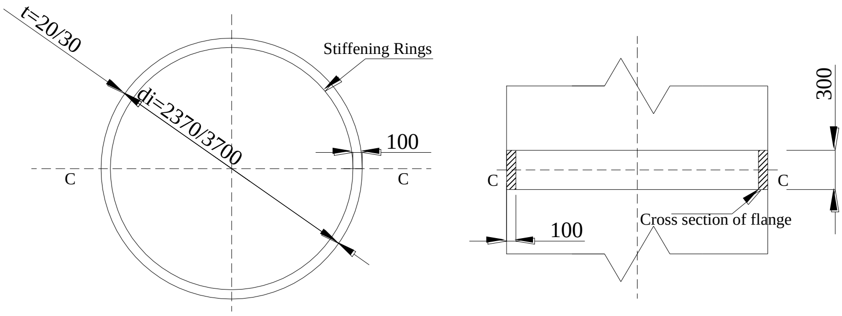

Fig. 2 Typical ring cross-sections of the 50m ring-stiffened tower (in mm)

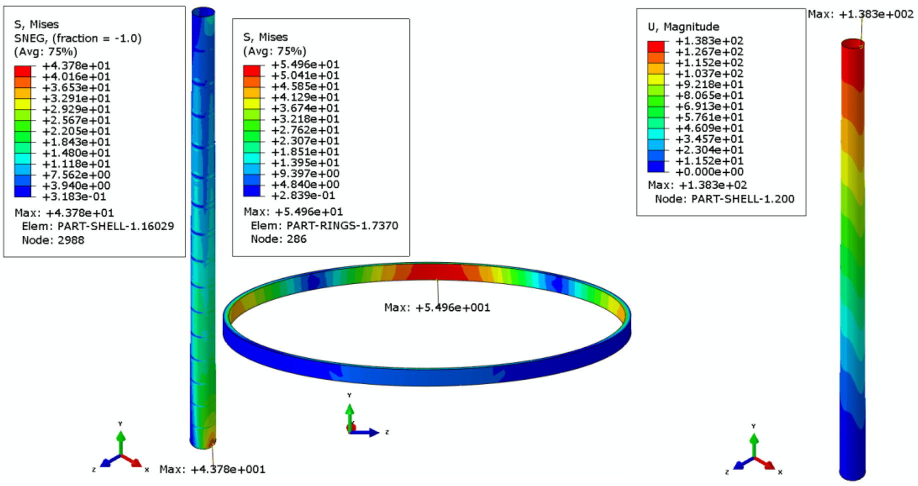

a. von Mises stress: shell b. von Mises stress: ring c. Horizontal sway

Fig. 3 The von Mises stress of shell and ring and the horizontal sway of the 150m ring-stiffened tower

Table 1 Shell thickness of the three heights of tower with stiffening rings

50m	Height zone	0-33.34m	33.34m-50m	
	Shell thickness (mm)	30mm	20mm	
150m	Height zone	0-50m	50m-100m	100m-150m
	Shell thickness (mm)	55mm	45mm	40mm
250m	Height zone	0 to100m	100m to 200m	200m to 250m
	Shell thickness (mm)	75mm	65mm	60mm

tower in terms of accelerations, stresses, deflections and rotations.

In this paper, three representative towers of 50m, 150m and 250m in height were considered stiffened alternatively with horizontal rings and vertical stiffeners. To explore the effect of vertical stiffeners on the enhancement of the structural response of towers, the strength and buckling behaviour of vertically and horizontally stiffened towers under wind loads were compared with each other where the mass of the stiffening rings was equal to that of the vertical stiffeners. The maximum von Mises stresses and horizontal sways of these towers with vertical stiffeners were compared with the corresponding towers with horizontal stiffening rings. The buckling modes and eigenvalues of the 50m, 150m and 250m vertically stiffened towers were also compared with those of the horizontally stiffened towers. A parametric study of the effect of the vertical stiffeners on the overall structural response of each tower was also performed, which led to some useful comments on the efficiency of the proposed stiffening technique.

2. Ring-stiffened towers

2.1 Model descriptions

Three ring-stiffened towers of various heights were considered and their structural analysis was performed using the Finite Element Method (FEM) based on the software of ABAQUS (2008). The geometric prototypes and the respective FEM models of the 50m, 150m and 250m towers with stiffening rings are shown in Fig. 1. The stiffening rings were uniformly distributed on the inner side of the tower walls. The spacing between two neighbouring rings in the 50m, 150m and 250m towers were 4167mm, 9375mm and 8621mm, respectively (Fig. 1). For the stiffening rings, the mid-section width and thickness in all three heights of tower were 100mm and 300mm, respectively (Fig. 2), and the Young's modulus, density and Poisson's ratio were 205GPa, 7.85g/cm^3 and 0.3, respectively. Thus, the masses of the stiffening rings of the 50m, 150m and 250m ring-stiffened towers are 24t, 78t and

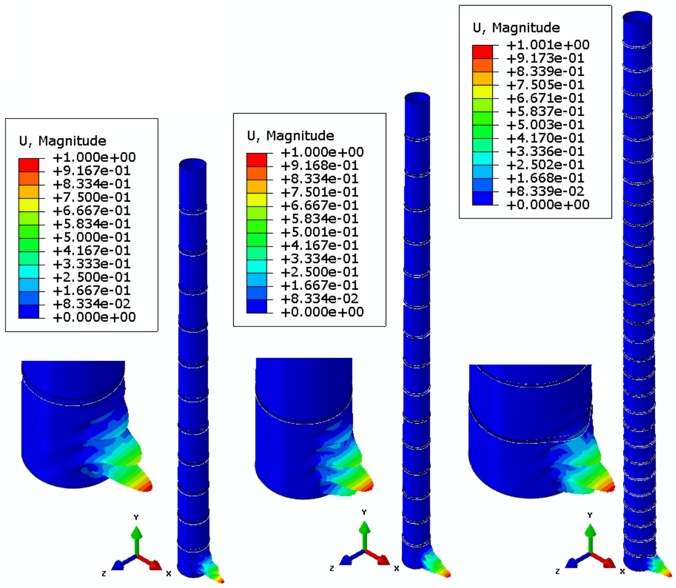

a. 50m ring-stiffened tower b. 150m ring-stiffened tower c. 250m ring-stiffened tower

Fig. 4 First local mode shape of the three towers with stiffening rings

Table 2 Maximum von Mises stresses and horizontal sways of the three heights of tower with stiffening rings

Height of tower (m)	Variables	Results
50	Max. horizontal sway (mm)	6.52
	Max. stress (MPa)	11.72
	Max. stress of shell (MPa)	11.72
150	Max. horizontal sway (mm)	138.26
	Max. stress (MPa)	54.96
	Max. stress of shell (MPa)	43.78
250	Max. horizontal sway (mm)	503.17
	Max. stress (MPa)	84.56
	Max. stress of shell (MPa)	73.09

241t, respectively. Concerning the FEM models, the tower walls and stiffening rings of the three heights of tower were simulated using S4R shell elements and C3D10R solid elements, after Hu *et al*. (2014). A tie restraint was employed to connect the tower walls with the stiffening rings, and the loading cases of the three heights of tower are based on the details provided by Hu *et al.* (2014). On the top of the tower, as the gravity centre of nacelle and rotor does not coincide with the geometric centre of the tower section leading to the eccentricity, the weight of the nacelle, together with the blades and the rotor, will induce the vertical force and moment that act on the top of the tower, therefore, for the weight of nacelle, blades and rotor, it could be simplified into the vertical force and moment in their corresponding FE models (Nguyena *et al*. 2015), which are 750kN and 400kNm for the 50m towers, respectively. As for 150m towers, the gravity of nacelle and rotor and their moment are 2300kN and 3550kN·m respectively. Whereas for 250m towers, the magnitude of moment and the vertical force are 9800kN·m and 3800kN.

The contour plots of the von Mises stress of the shell and the ring, and the horizontal sway of the 150m ring-stiffened tower are shown in Fig. 3. The maximum von Mises stress in the shell of the 150m tower is 43.78MPa and occurs at the vicinity of the tower base, whereas the maximum horizontal sway of the same tower is 138.26mm at the top. The maximum von Mises stresses and horizontal sways of the 50m, 150m and 250m ring-stiffened towers are shown in Table 2. The maximum von Mises stress and the horizontal sway of the 50m tower are 11.72MPa and 6.52mm, respectively. For the 250m ring-stiffened towers, the maximum von Mises stresses in the ring and the shell are 84.56MPa and 73.09MPa, respectively and the maximum horizontal sway is 503.17mm (Table 2).

2.2 Buckling analysis of ring-stiffened towers

The stiffeners are added to the inner shell of the tower in order to supress the local buckling of the cylindrical shell. This way, the buckling capacity of steel tubular wind turbine towers is enhanced due to the presence of stiffeners. In this section, a linear buckling analysis is performed to study the buckling modes and the critical buckling loads of the three heights of tower. Axial, transverse and torsional loads act at the top of the tower (Hu *et al. 2014*) , and these are equivalent to respectively, the weight of the nacelle, the blades and the rotor, f_n, a horizontal force, f_w from the manufacturer's data and the bending moment, f_m from the weight of the nacelle eccentricity relative to the tower axis. In addition, the wind pressure, p is distributed along and around the surface of the tower wall. The loading states for each height case are combined into the expression:

$$f = f_n + f_m + f_w + p \tag{1}$$

The first local mode shapes of the ring-stiffened towers at the three heights are shown in Figure 4, and the absolute values of the first buckling eigenvalues of the corresponding tower height are displayed in Table 3.

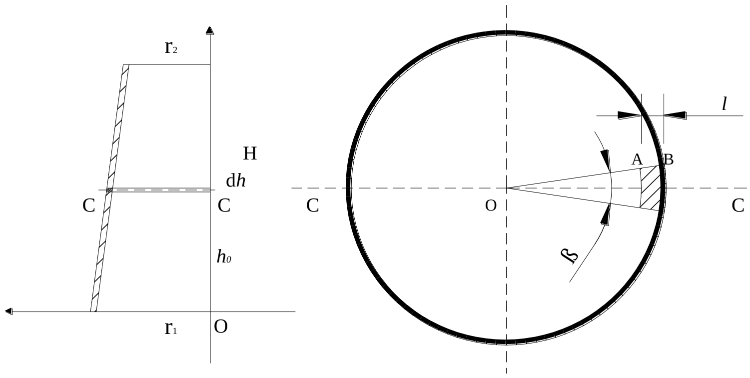

a. Longitudinal profile of tower b. Cross section

Fig. 5 Profile of the wind turbine tower in two perpendicular planes

Table 3 First buckling eigenvalues of the 50m, 150m and 250m towers

Height of tower (m)	50m	150m	250m
First eigenvalue	79.06	29.8	12.48

The first mode shapes of the three heights of tower are all local buckling in the positive direction of the x axis and occur in the vicinity of the tower bases, as shown in Fig. 4. The first buckling eigenvalues of the 50m, 150m and 250m towers are 79.058, 29.8 and 12.48, respectively. The negative magnitudes indicate that the direction of the local buckling modes is opposite to the load direction.

3. Vertically stiffened towers

3.1 On the mass of the vertical stiffeners

To study the effect of vertical stiffeners on the structural response of wind towers, the maximum von Mises stress and horizontal sway of each height case should be compared where the mass of the vertical stiffeners is equal to that of the stiffening rings of the corresponding wind turbine tower. The formulas for the mass of each vertical stiffener can be obtained using the mathematical model presented schematically in Fig. 5. Figure 5 shows the geometric profile of the tower, showing the longitudinal section and the cross section. The cross sectional radii of the tower at the base and at the top of the vertical stiffener are r_1 and r_2 respectively. dh is the differential height of the cross-section C-C at height, h_0 from the bottom of the vertical stiffener to the cross-section C-C (Fig. 5a). The central angle of the arc of the vertical stiffener at this point is β, and the thickness of the vertical stiffener at this point is l, as shown in Fig. 5b.

According to the geometry of the tower (Fig. 5), the following formulas are obtained:

$$r_{OB} = \frac{r_2 - r_1}{H} \cdot h + r_1 \quad (2)$$

$$r_{OB} - r_{OA} = l \quad (3)$$

$$S = 0.5 \cdot \beta \cdot r_{OB}^2 - 0.5 \cdot \beta \cdot r_{OA}^2 \quad (4)$$

Table 4 Thickness of the vertical stiffeners of the 50m towers

Types of vertical stiffeners	Thickness of vertical stiffeners (mm)		
	tower *a*	tower *b*	tower *c*
V_i	72	49	18
V_{ii}	59	39	14
V_{iii}	49	32	12

where S is the cross-sectional area of the vertical stiffener at the cross-section C-C; r_{OA} is the inner radius of the vertical stiffener; r_{OB} is the outer radius of the vertical stiffener; H is the height of the vertical stiffener; and ρ is the density of steel.

According to Equations (2- 4), the mass of each vertical stiffener can be obtained by Equation (5):

$$m = \rho \cdot \int_0^H S dh = 0.5 \cdot \rho \cdot \beta \cdot l \cdot H \cdot (r_1 + r_2 - l) \quad (5)$$

3.2 Model descriptions

3.2.1 50m towers

The 50m tower contains eight, sixteen or thirty-two vertical stiffeners uniformly distributed on the inner side of the cylindrical tower as shown in Fig. 6, and referred to as "tower *a*", "tower *b*" and "tower *c*". The height of each vertical stiffener is 50m from the bottom to the top of the tower as shown in Fig. 6a. The central angle, β of each vertical stiffener was selected to be 4°, 5° or 6° (referred to as "V_i", "V_{ii}" and "V_{iii}"). As the diameter of the 50m tower varies linearly from 3.7m at the base to 2.37m at the top, the mid-arc-length of the cross-section of each vertical stiffener also varies linearly. The wall thickness of the 50m towers *a*, *b* and *c* is identical to that of the 50m ring-stiffened tower. For wind loading, the magnitudes for the 50m towers *a*, *b* and *c* are identical to those described by Hu *et al.* (2014). A typical cross-section and vertical stiffener distribution of the 50m tower *a* is shown in Fig. 7. The tower wall was simulated using S4R shell elements and the vertical stiffeners were simulated using C3D10 solid elements.

According to the model described above, the mass of the 50m ring-stiffened tower is 24t, and the maximum von Mises stress and horizontal sway of the 50m ring-stiffened

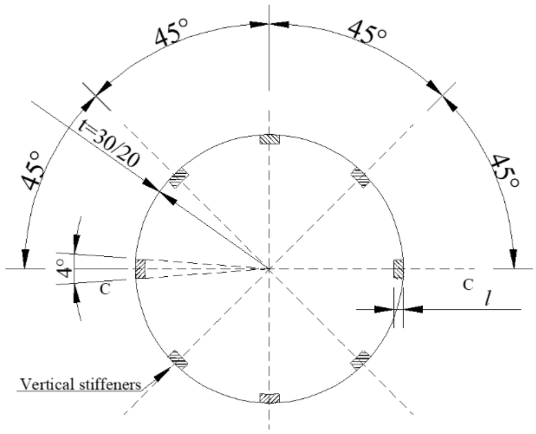

Fig. 7 Typical cross-section of the 50m tower *a* with V_i

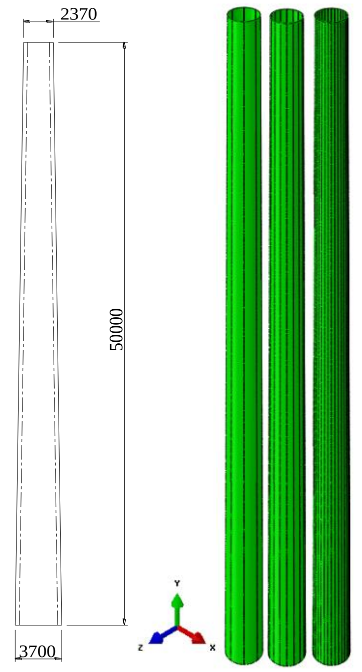

a. Geometrical data b. FEM model

Fig. 6 Prototypes of the 50m towers *a*, *b* and *c* (mm)

tower are 11.72MPa and 6.52mm, respectively. To analyse the effect of the vertical and horizontal stiffeners, the mass of the vertical stiffeners has been selected to be equal to that of the stiffening rings of the 50m ring-stiffened tower. Therefore, the thickness of the stiffeners in the three vertical stiffened cases can be obtained by means of the given parameters and Equation (5), and the magnitudes of the vertical stiffeners are shown in Table 4. Specifically, the thicknesses *l* of the 50m towers *a*, *b* and *c* with V_i are 72mm, 49mm and 18mm, respectively. The thicknesses *l* of the 50m towers *a*, *b* and *c* with V_{ii} are 59mm, 39mm and 14mm, respectively, and the thicknesses *l* of the 50m towers *a*, *b* and *c* with V_{iii} are 49mm, 32mm and 12mm, respectively.

3.2.2 150m towers

The geometry and the FEM model of the 150m towers with vertical stiffeners are depicted in Fig. 8. The models of

Table 5 Thickness of the vertical stiffeners of the 150m towers

Types of vertical stiffeners	Thickness of vertical stiffeners (mm)		
	Tower *a*	Tower *b*	Tower *c*
V_i	68	45	33
V_{ii}	45	30	22
V_{iii}	33	22	17

the 150m tower with eight, twelve or sixteen vertical stiffeners are shown in Fig. 8b and are referred to as "tower *a*", "tower *b*" and "tower *c*". The sixteen vertical stiffeners are uniformly distributed on the inner side of the tower as shown in Fig. 9. The diameters of the 150m towers *a*, *b* and *c* reduce linearly from 8.5m at the base to 5.7m at the top. The length of each vertical stiffener of the 150m towers is 150m. The central angles, β of each vertical stiffener are 2°, 3° and 4° respectively, (referred to as "V_i", "V_{ii}" and "V_{iii}"). The masses of the vertical stiffeners for the 150m towers *a*, *b* and *c* are all equal to those of the 150m ring-stiffened tower. Therefore, the thicknesses *l* of the vertical stiffeners of the 150m towers with V_i are 68mm, 45mm and 33mm respectively, obtained by applying Equation (5). The thicknesses of the 150m towers with V_{ii} are 45mm, 30mm and 22mm respectively, and those of the 150m towers with V_{iii} are 33mm, 22mm and 17mm respectively, as shown in Table 5. The wall thickness of the 150m towers *a*, *b* and *c* is 55mm from the height of 0m to 50m, 45mm from the height of 50m to 100m, and 40mm from the height of 100m to 150m. The loading states of the 150m towers *a*, *b* and *c* are identical to those described by Hu *et al.* (2014).

3.2.3 250m towers

The geometrical data and the FE models of the 250m towers with eight, sixteen or thirty-two vertical stiffeners (referred to as "tower *a*", "tower *b*" and "tower *c*") are shown in Fig. 10. The diameter of the 250m towers reduces linearly from 14m at the base to 9.5m at the top. The vertical stiffeners of the 250m towers *a*, *b* and *c* are equally distributed around the circumference, from the base to the top of the tower as shown in Fig. 11. For each vertical stiffener, the central angles, β of the vertical stiffener are 1° 1.5° and 2° respectively (referred to as "V_i", "V_{ii}" and "V_{iii}") as shown in Fig. 11. The mass of the stiffeners for

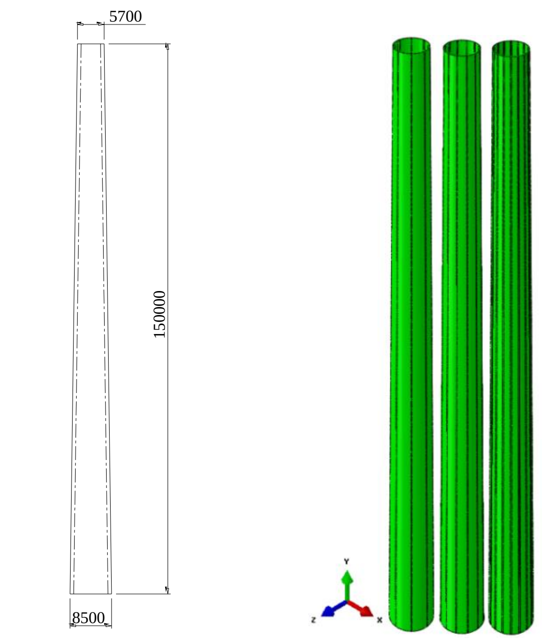

a. Geometrical data b. FE model

Fig. 8 Prototypes of the 150m towers *a*, *b* and *c* (mm)

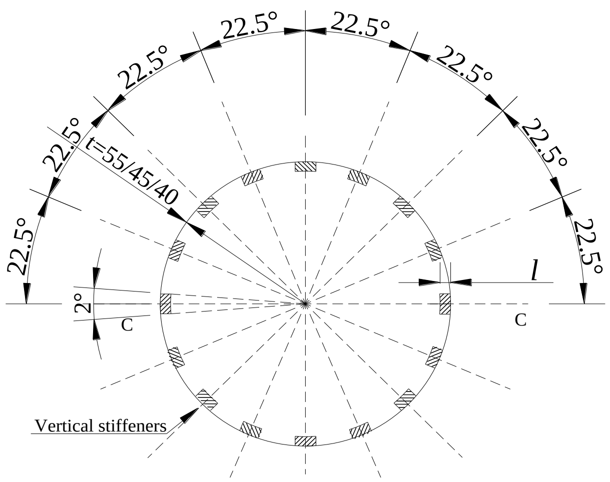

Fig. 9 Typical cross-section of the 150m tower *c* with V_i

Table 6 Thickness of the vertical stiffeners of the 250m towers

Type of vertical stiffeners	Thickness of vertical stiffeners (mm)		
	Tower *a*	Tower *b*	Tower *c*
V_i	152	75	38
V_{ii}	101	50	25
V_{iii}	75	38	19

each of the three vertical stiffened towers is 241.34t, equal to that of the stiffening rings of the 250m ring-stiffened tower. According to Equation (5), the thicknesses of the vertical stiffeners of the 250m towers with V_i are 152mm, 75mm and 38mm respectively, and those of the 250m tower with V_{ii} are 101mm, 50mm and 25mm, respectively. The thicknesses of the vertical stiffeners for the 250m tower with V_{iii} are 75mm, 38mm and 19mm, respectively, as shown in Table 6. The wall thickness of the 250m towers

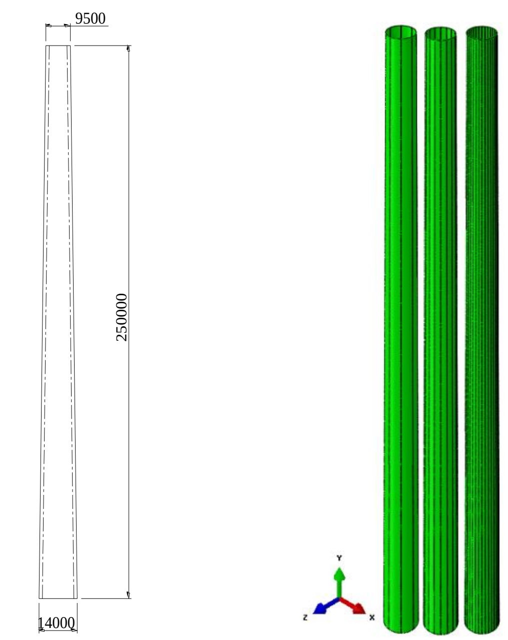

a. Geometrical data b. FE model

Fig. 10 Prototypes of 250m towers *a*, *b* and *c* (mm)

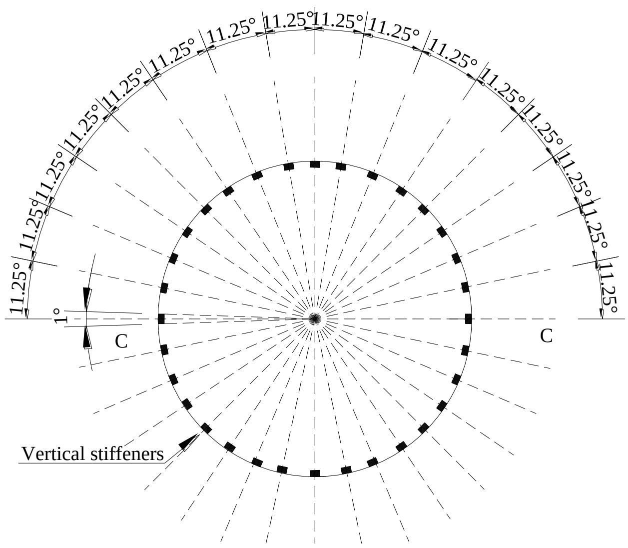

Fig. 11 Typical cross-section of the 250m tower *b* with V_i

a, *b* and *c* is 75mm from the height of 0m to 100m, 65mm from the height of 100m to 200m, and 60mm from the height of 200m to 250m. The wall thickness and the wind loadings of the 250m towers *a*, *b* and *c* are identical to those of the 250m ring-stiffened tower.

3.3 Effect of the number of vertical stiffeners

Figure 12 shows the contour plots of the von Mises stresses and the horizontal sways of the 50m towers *a* with V_i. The maximum von Mises stresses and horizontal sways of the 50m, 150m and 250m towers *a*, *b* and *c* are shown in Table 7. The maximum von Mises stresses of the 50m towers *a*, *b* and *c* with V_i are 23.23MPa, 22.68MPa and 20.32MPa, respectively. The maximum horizontal sways of the 50m towers *a*, *b* and *c* with V_i are 5.683mm, 5.617mm

Table 7 Maximum von Mises stress and horizontal sway of the 50m, 150m and 250m towers

Type of vertical stiffeners	Type of tower	Maximum von Mises stress (MPa)			Maximum horizontal sway (mm)		
		50m	150m	250m	50m	150m	250m
V_i	*a*	23.23	48.63	83.03	5.68	136.2	505.5
	b	20.32	47.82	82.35	5.60	134.5	504.9
	c	16.68	47.1	81.54	5.46	134.6	504.9
V_{ii}	*a*	23.02	47.38	82.29	5.643	134.6	499.1
	b	17.43	47.14	80.79	5.54	134.5	492.9
	c	16.19	46.02	79.33	5.46	134.5	492.6
V_{iii}	*a*	22.07	47.09	81.53	5.64	134.8	493.5
	b	16.61	46.95	80.07	5.48	134.7	492.8
	c	15.64	46.20	78.91	5.43	134.4	492.6

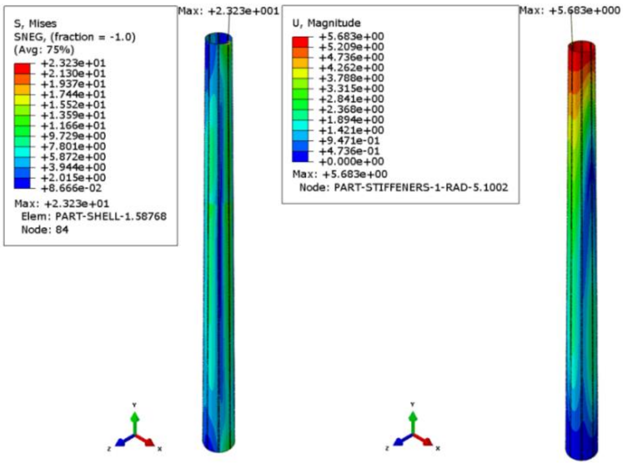

Fig. 12 Contour plots of 50m tower *a* with V_i

and 5.601mm. The maximum von Mises stresses of the 150m towers *a*, *b* and *c* are 48.63MPa, 47.82MPa and 47.1MPa respectively, occurring in the vicinity of the base of the 150m towers. However, the maximum horizontal sways of the 150m towers *a*, *b* and *c* appear at the top of the towers, with magnitudes of 136.2mm, 134.5mm and 134.6mm respectively. The maximum von Mises stresses of the three 250m vertically stiffened towers are 83.03MPa, 82.35MPa and 81.54MPa respectively, which are less than those in the rings of the 250m ring-stiffened tower previously described. The maximum horizontal sways of the 250m towers *a*, *b* and *c* are 505.5mm, 504.9mm and 504.9mm respectively, which are slightly greater than the 503.17mm maximum horizontal sway of the 250m ring-stiffened tower. The horizontal sways of the three heights of tower with vertical stiffeners increase as the height of the tower increases, as shown in Fig. 12.

As the mass of the vertical stiffeners has been selected to be equal to that of the stiffening rings, the efficiency in strength variation of the 50m towers can be obtained by comparing the maximum von Mises stress and horizontal sway of the 50m vertically- and horizontally-stiffened towers. The maximum von Mises stresses of the three vertically stiffened towers are all greater than those of the 50m towers with stiffening rings, but the maximum horizontal sways of the towers *a*, *b* and *c* are less than those of the horizontally stiffened towers as shown in Table 7. Therefore, the use of stiffening rings appears to be a more efficient way to strengthen the tower compared to the use of vertical stiffeners in the case where the mass of the vertical stiffeners is equal to that of the stiffening rings.

For the 150m tower with stiffening rings, the maximum von Mises stresses in the rings and shell are 54.95MPa and 43.78MPa respectively, and its maximum horizontal sway is 138.26mm as shown in Table 2. According to Table 7, the maximum von Mises stresses of the 150m towers *a*, *b* and *c* are all less than the maximum von Mises stresses in the rings, and are all close to those in the shell of the 150m horizontally stiffened tower. The maximum horizontal sways of 150m towers *a*, *b* and *c* are less than those of the 150m ring-stiffened tower. Therefore, vertical stiffeners effectively increase the strength of the 150m towers *a*, *b* and *c* compared with stiffening rings which have the same mass as the vertical stiffeners.

As shown in Table 7, the maximum von Mises stresses and horizontal sways of the 250m towers *a*, *b* and *c* reduce as the number of vertical stiffeners increases in the case where the mass of the vertical stiffeners is equal to that of the stiffening rings of the 250m tower with stiffening rings. For the 250m towers *a*, *b* and *c* with V_{ii} and V_{iii}, the maximum von Mises stresses and horizontal sways are less than those of the 250m ring-stiffened tower. Therefore, the vertical stiffeners seem to be a better choice in increasing the strength of towers than the horizontal stiffening rings with the same mass as the vertical stiffeners, when comparing the 250m towers.

For each vertical stiffener, the maximum von Mises stresses and horizontal sways of the 50m, 150m and 250m towers *a*, *b* and *c* are shown in Table 7. The maximum von Mises stresses and horizontal sways of the 50m, 150m and 250m towers *a*, *b* and *c* with respect to the numbers of vertical stiffeners are plotted in Figs. 13 to 15. The x axis represents the number of vertical stiffeners in the three heights of tower, and the y axis refers to the maximum von Mises stresses and the horizontal sways of the three heights of tower.

As shown in Figs. 13-15, the maximum von Mises stresses of the 50m, 150m and 250m vertically stiffened towers *a*, *b* and *c* reduce as the number of vertical stiffeners increases, where the stiffeners have the same mass as the horizontal rings. The maximum horizontal sways of the

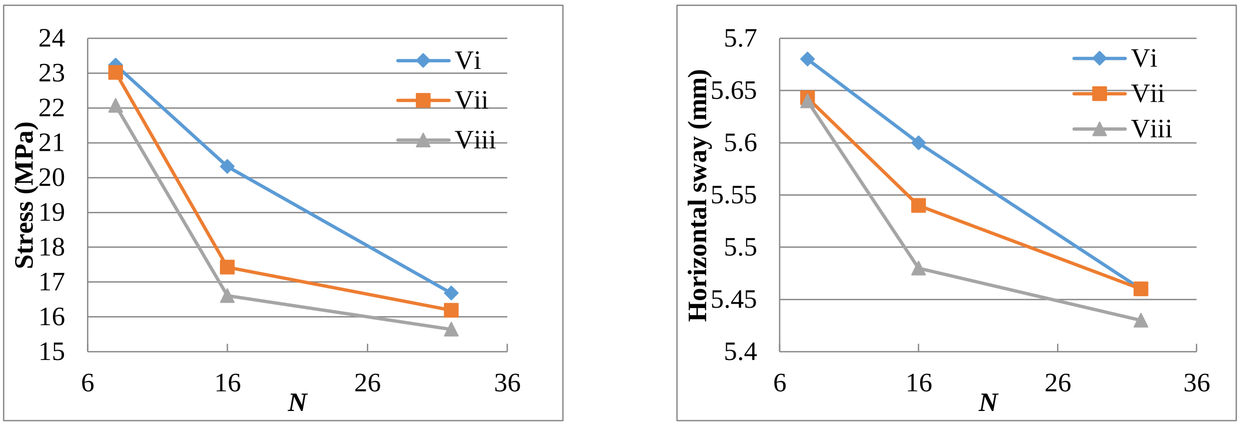

Fig.13 Maximum von Mises stress and horizontal sway of the 50m towers with V_i, V_{ii} and V_{iii}

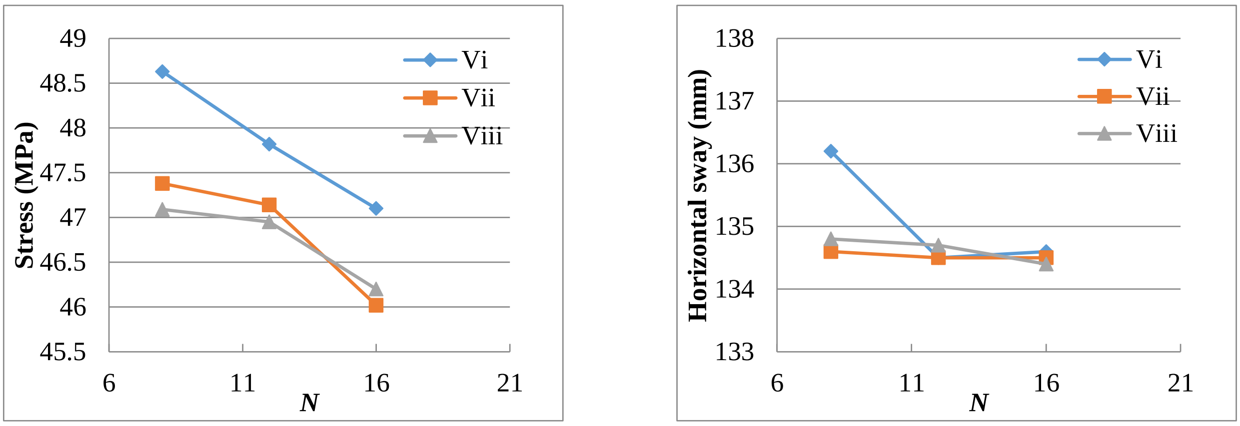

Fig. 14 Maximum von Mises stress and horizontal sway of 150m towers with V_i, V_{ii} and V_{iii}

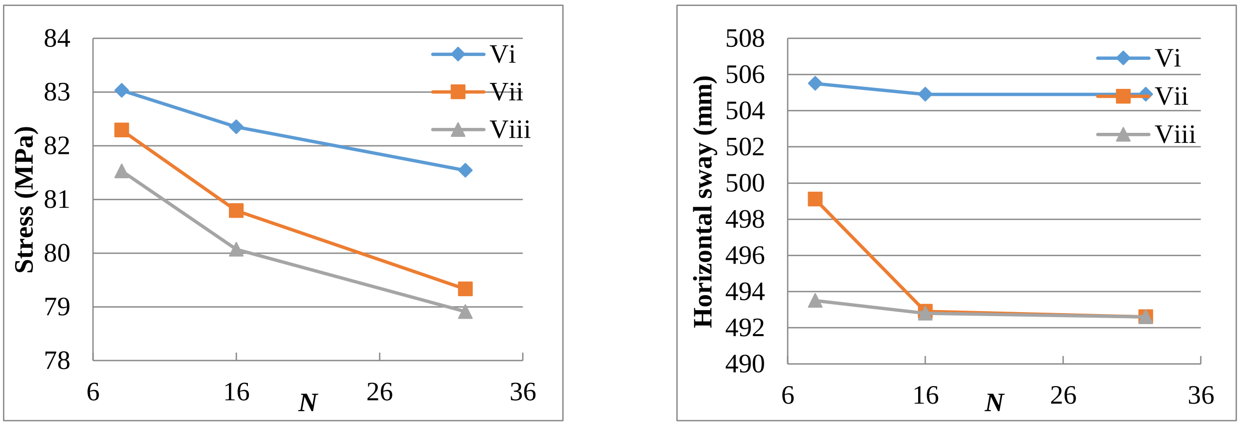

Fig. 15 Maximum von Mises stress and horizontal sway of the 250m towers with V_i, V_{ii} and V_{iii}

50m, 150m and 250m towers with V_i, V_{ii} and V_{iii} also reduces as the number of vertical stiffeners increases. The maximum horizontal sways of the 50m towers *a*, *b* and *c* are almost identical. Therefore, the strength of the 50m towers increases as the number of vertical stiffeners increases, where the masses of the horizontal and vertical stiffeners are equal to each other as shown in Table 7 and Figs. 13-15.

3.4 Effect of the central angle of the vertical stiffeners

Considering the same prototype of the tower stiffened with vertical stiffeners, the central angle, β of the vertical stiffeners is considered to be the design variable in terms of equation (5), and its effect on the strength of the towers has been studied. The maximum von Mises stresses and horizontal sways of the 50m, 150m and 250m towers *a*, *b* and *c* are depicted in Figs. 16-18. The horizontal axis refers to the central angle of the arc of each vertical stiffener for each tower height, and the vertical axis represents the maximum von Mises stresses and horizontal sways of the 50m, 150m and 250m towers *a*, *b* and *c*.

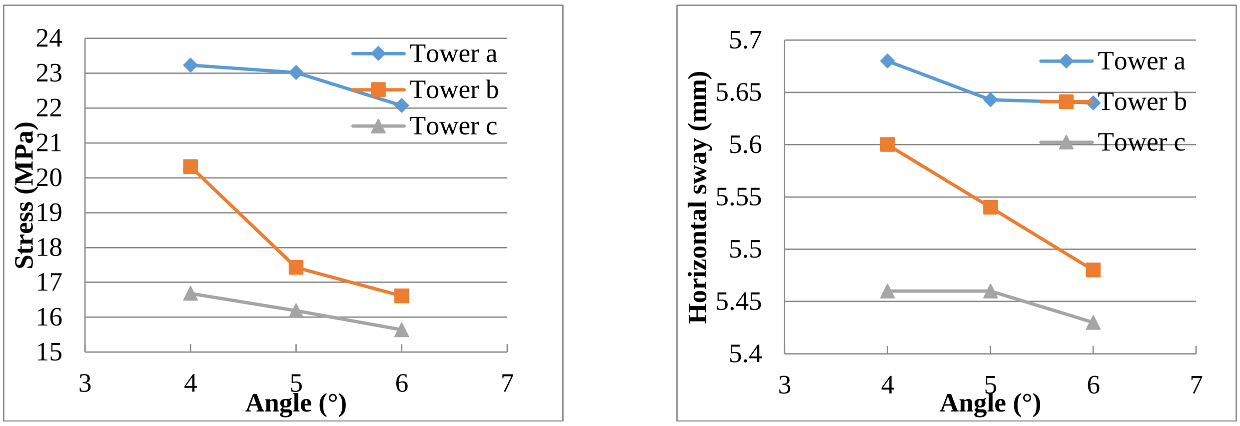

Fig. 16 Maximum von Mises stress and horizontal sway of the 50m towers *a*, *b* and *c*

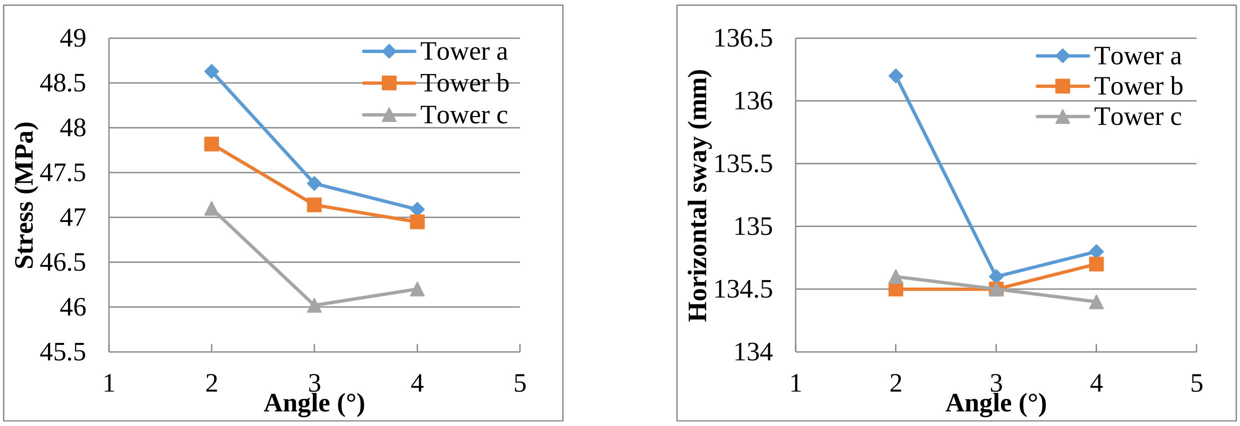

Fig. 17 Maximum von Mises stress and horizontal sway of the 150m towers *a*, *b* and *c*

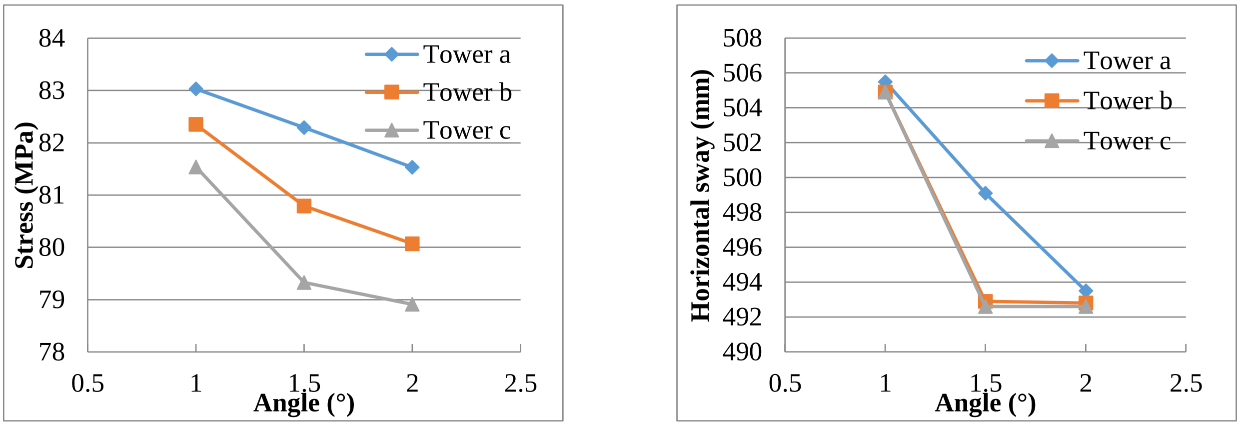

Fig. 18 Maximum von Mises stress and horizontal sway of the 250m towers *a*, *b* and *c*

According to Fig. 16, the maximum von Mises stress reduces, and the maximum horizontal sway of the 50m tower *a*, *b* and *c* increases with an increase in the central angle, β of the cross-sectional arc of each vertical stiffener. Therefore, the strength of the 50m towers increases with an increase in the central angle, β of the cross-sectional arc of each vertical stiffener.

For the 150m towers, the maximum von Mises stresses and horizontal sways of towers *a*, *b* and *c* are shown in Fig. 17. The maximum von Mises stresses of the 150m tower types *a* and *b* reduce with an increase in the central angle of each vertical stiffener. The maximum von Mises stress of the 150m tower *c* with V_{ii} is less than those of the 150m tower *c* with V_i and V_{iii}. Moreover, the maximum von Mises stresses of the 150m tower *c* with V_{ii} and V_{iii} are similar. The maximum von Mises stress of the 150m towers *a*, *b* and *c* decreases with an increase in the central angle of the vertical stiffeners. The maximum horizontal sway of the 150m tower *a* with V_{ii} is less than that of the 150m tower *a* with V_{ii} and V_{iii}, and the maximum horizontal sways of the 150m tower *b* increase with an increase in the central angle of the vertical stiffener. However, the maximum horizontal sway of the 150m tower *c* reduces as the central angle of the vertical stiffener increases. As the magnitudes of the

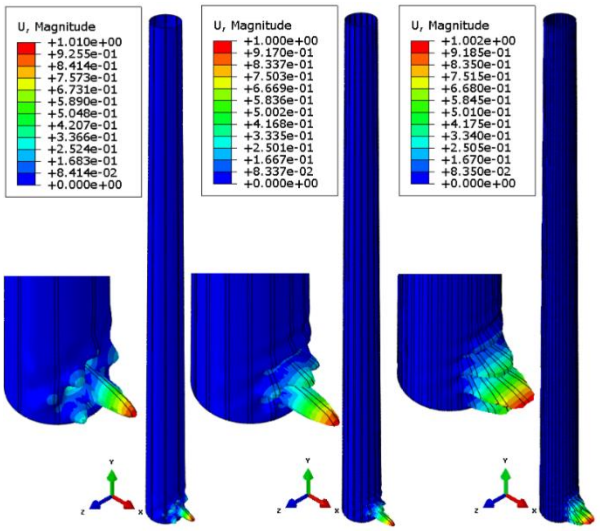

Fig. 19 First local buckling modes of the 50m towers *a*, *b* and *c* with V_i

maximum horizontal sway are almost identical for the 150m towers *a*, *b* and *c*, the strength variation of the 150m tower can be determined by considering the variation of the maximum von Mises stress. Thus, the strength of the 150m tower can be enhanced by increasing the central angle β of the vertical stiffener.

The maximum von Mises stresses and the horizontal sways of the 250m towers *a*, *b* and *c* with respect to the central angle, β of each vertical stiffener are depicted in Fig. 18. The maximum von Mises stresses and horizontal sways of the 250m towers *a*, *b* and *c* reduce as the central angle, β of each vertical stiffener increases. The maximum horizontal sways of the 250m tower *b* and *c* show a similar trend as the central angle, β of each vertical stiffener increases. It is concluded that an increase in the central angle, β of each vertical stiffener significantly improves the strength of the 250m towers.

3.5 Buckling analysis of vertically stiffened towers

A linear buckling analysis was performed to investigate the effect of the vertical stiffeners on the stability of the 50m, 150m and 250m vertically stiffened towers under wind loadings. The load states include axial, transverse and torsional loads at the top of the tower and wind loading around the circumference. The thickness, *l* and the central angle, β of each vertical stiffener were considered as design parameters, and the effect of the various vertical stiffeners on the buckling behaviour of the 50m towers were obtained. Additionally, the local buckling modes and the eigenvalues of the 50m ring-stiffened tower are also compared with those of the 50m towers *a*, *b* and *c* to estimate a better approach to strengthen the 50m towers.

The local buckling modes of the 50m towers *a*, *b* and *c* with V_i are displayed in Fig. 19. As can be seen, the first local buckling modes of the 50m towers *a*, *b* and *c* with V_i all occur in the vicinity of the base of the towers. The absolute values of the buckling eigenvalues of the 50m, 150m and 250m towers *a*, *b* and *c* are presented in Table 8. The buckling modes of the 150m and 250m horizontally stiffened towers are also local buckling and occur in the vicinity of the tower bases.

The buckling eigenvalues of the 50m, 150m and 250m towers with respect to each central angle, and the number of vertical stiffeners are presented in Figs. 20-22. For each central angle, β of the arc of the vertical stiffener, the buckling eigenvalues of the 50m towers *a*, *b* and *c* increase with the number of vertical stiffeners, as shown in Fig. 20. For each number of vertical stiffeners, the buckling eigenvalues of the 50m towers *b* and *c* increase as the central angle, β of the vertical stiffener increases. However,

Table 8 First buckling eigenvalues of the 50m, 150m and 250m towers *a*, *b* and *c*

Type of vertical stiffeners	Type of tower	Eigenvalues 50m	150m	250m
V_i	*a*	68.03	28.01	18.79
	b	67.32	28.94	19.42
	c	79.93	29.67	19.81
V_{ii}	*a*	62.59	28.63	18.69
	b	71.78	29.75	19.65
	c	83.29	30.75	20.46
V_{iii}	*a*	57.74	29.38	18.59
	b	73.85	30.21	19.91
	c	85.91	30.88	20.69

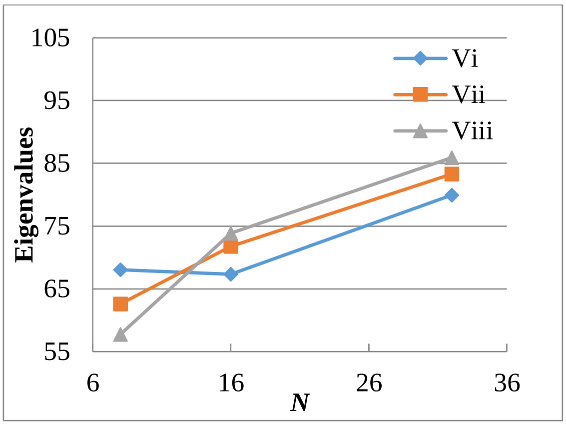

a. Eigenvalues of the 50m towers with V_i, V_{ii} and V_{iii}

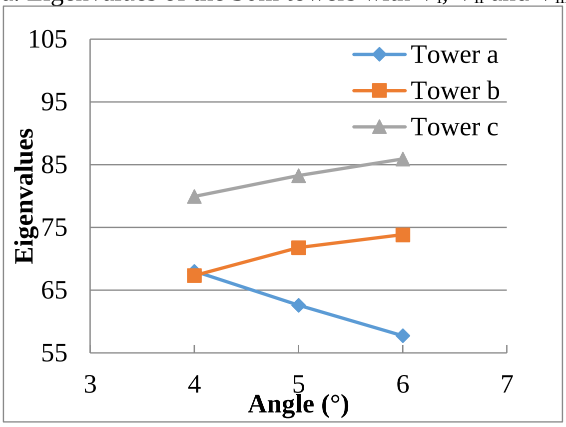

b. Eigenvalues of the 50m towers *a*, *b* and *c*

Fig. 20 Local buckling eigenvalues of the 50m towers

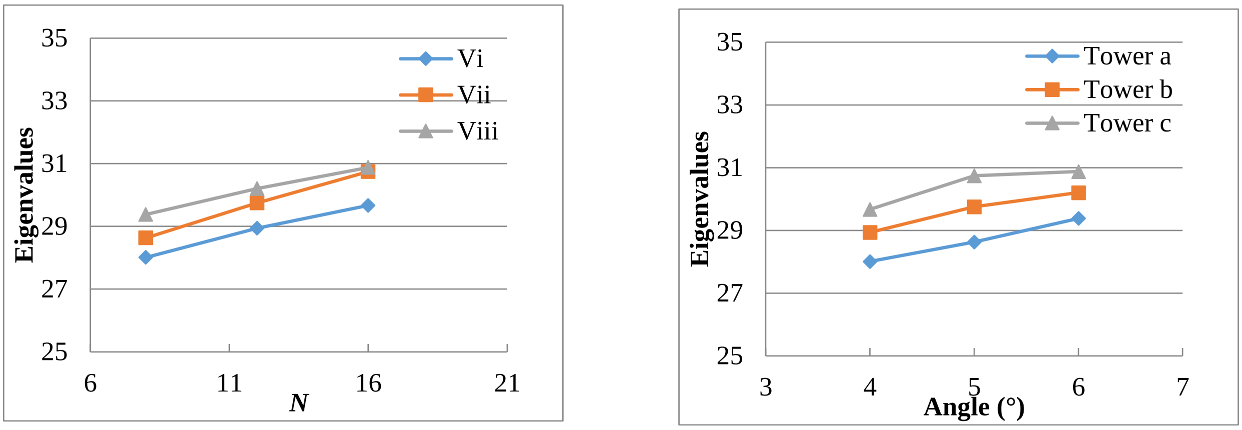

a. Eigenvalues of 150m towers with V_i, V_{ii} and V_{iii} b. Eigenvalues of the 150m towers *a*, *b* and *c*

Fig. 21 Local buckling eigenvalues of the 150m towers

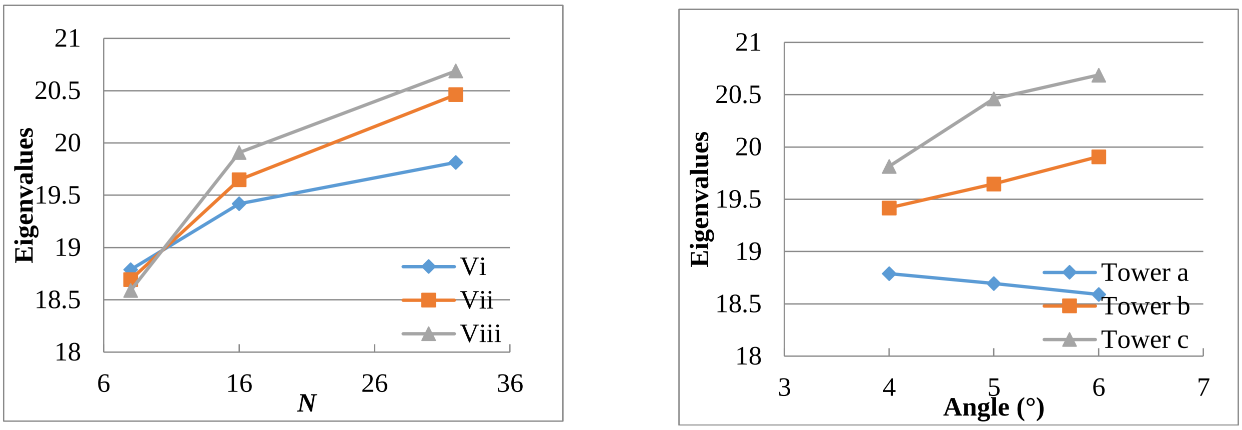

a. Eigenvalues of 50m towers with V_i, V_{ii} and V_{iii} b. Eigenvalues of the 50m towers *a*, *b* and *c*

Fig. 22 Local buckling eigenvalues of the 250m towers

the buckling eigenvalues of the 50m towers *a* reduce as the central angle of the vertical stiffeners increases. Compared with the 50m ring-stiffened towers, the absolute value of the corresponding buckling eigenvalues of the vertically stiffened 50m towers *a* and *b* (shown in Table 8) are less than the eigenvalue of the 50m ring-stiffened tower (Table 3), but the absolute eigenvalues of the 50m towers *c* are greater than those of the 50m ring-stiffened tower. Thus, the stability strength of the 50m towers can be improved more efficiently by using vertical stiffeners which have the same mass as the stiffening rings.

For the 150m ring-stiffened towers, the first local buckling eigenvalues are shown in Fig. 21. The first local buckling eigenvalues of the 150m towers increase as the number and the central angle of the vertical stiffeners increases. The absolute values of the eigenvalues of the 150m towers *b* and *c* with V_{iii} are greater than those of the 150m horizontally stiffened tower. Therefore, using vertical stiffeners of the same mass as the stiffening rings is a more appropriate option to strengthen the stability of the 150m towers than using stiffening rings.

Table 8 shows the absolute values of the buckling eigenvalues of the 250m towers, and the buckling eigenvalues are given in Fig. 22. The eigenvalues of the 250m towers, for each central angle β of the vertical stiffeners, increase with an increase in the number of vertical stiffeners. The eigenvalues of the 250m towers, for each number of vertical stiffeners, increase as the central angle β of the vertical stiffeners increases. In other words, the stability of the 250m vertically stiffened towers increases as the number and the central angle of the vertical stiffeners increase. Vertical stiffeners can be utilised as a better design approach to improve the stability of the 250m towers than an approach using stiffening rings, where the mass is equal to that of the vertical stiffeners.

4. Conclusions

In this paper, the number of vertical stiffeners and the central angle of each vertical stiffener for the three height cases was considered as design parameters. In each case, the mass of the vertical stiffeners is equal to the mass of the stiffening rings that would have employed otherwise in the same towers. The effect of vertical stiffeners and of horizontal rings on the structural response of these towers under wind loading is compared, and a parametric study with respect to the vertical stiffeners was carried out performed. It is concluded that the use of stiffening rings is a more efficient approach than the use of vertical stiffeners for the low height towers in terms of strength performance enhancement, whereas for the intermediate and higher tower, vertical stiffeners are a more efficient way to enhance the strength of towers than horizontal stiffening rings of equal mass. Moreover, the strength of all tower heights is increased with an increase in the number and the central angle of the vertical stiffeners.

Concerning the buckling analysis, the buckling strength of the low height towers with more vertical stiffeners increases as the quantity and the central angle β of the vertical stiffeners increases. The buckling strength of the low height towers with fewer vertical stiffeners reduces as the central angle β of the vertical stiffeners increases and as the number of vertical stiffeners is reduced. However, for the intermediate and high towers, their buckling strength increases as the number and the central angle of the vertical stiffeners increases. The use of vertical stiffeners is a more efficient approach to enhance the stability of the low, intermediate and high towers than the use of horizontal rings.

For the future work, environmental loads of offshore wind turbines with monopile are more complex than the onshore ones including higher average wind velocity and wave loadings. This makes the development of a new tall offshore tower model imperative for their analysis and design. In particular, the structural response of hyper tall offshore wind turbine towers under combined wind and waves, as well as their fatigue performance should be considered as significant potential research topics.

Acknowledgements

The first author acknowledges with thanks the research financial support provided by the China Scholarship Council (CSC) and China Postdoctoral funding (No. BR0100020), National Natural Science Foundation of China (No. 51808335). The financial support of the present research activity by the European Union's Horizon 2020 Research and Innovation Programme under the Marie Sklodowska-Curie Grant Agreement No 793316 is also gratefully acknowledged.

References

ABAQUS (2008), ABAQUS/Standard and ABAQUS/Explicit-Version 6.8-1. Abaqus Theory Manual, Dassault System.

Adhikaria, S. and Bhattachary, S. (2017), "Dynamic analysis of wind turbine towers on flexible foundations", *Shock. Vib.*, **19**, 37-56. https://doi.org/10.3233/SAV-2012-0615.

Alonso-Martineza M., Adamb J.M., Alvarez-Rabanala F.P., Coz Díaz J.J. (2019), "Wind turbine tower collapse due to flange failure: FEM and DOE analyses", *Eng. Failure Anal.*, **104**, 932-949. https://doi.org/10.1016/j.engfailanal.2019.06.045.

Baniotopoulos, C. C. and Stathopoulos T. (2007), *Wind Effects on Buildings and Design of Wind-Sensitive Structures*, Springer Wien, New York, NY, USA.

Baniotopoulos, C., Borri C. and Stathopoulos T. (2011), *Environmental Wind Engineering and Design of Wind Energy Structures*, CISM Courses and Lectures Udine, Springer Verlag, Italy.

Bray, F.M. and Egle, D.M. (1970), "An experimental investigation of the free vibration of thin cylindrical shells with discrete longitudinal stiffening", *J. Sound Vib.*, **12**(2), 153-164. https://doi.org/10.1016/0022-460X(70)90085-4.

Chen, J.F. and Rotter, J.M. (1998), "Effective cross sections of asymmetric rings on cylinderical shells", *J. Struct. Eng.*, **124**(9), 1074-1080. https://doi.org/10.1061/(ASCE)0733-9445(1998)124:9(1074).

Gong, J., Tao, J., Zhao, J., Zeng, S. and Jin, T. (2013), "Effect of top stiffening rings of open top tanks on critical harmonic settlement", *Thin-Wall. Struct.*, **65**, 62-71. https://doi.org/10.1016/j.tws.2013.01.011.

Hu, Y., Baniotopoulos, C. and Yang, J. (2014), "Effect of internal stiffening rings and wall thickness on the structural response of steel wind turbine towers", *Eng. Struct.*, **81**(81), 148-161. https://doi.org/10.1016/j.engstruct.2014.09.015.

Hull, A.J. (2012), "Elastic response of a cylinder containing longitudinal stiffeners", *J. Sound Vib.*, **331**(3), 588-604. https://doi.org/10.1016/j.jsv.2011.09.012.

Iwicki, P., Wójcik, M. and Tejchman, J. (2011), "Failure of cylindrical steel silos composed of corrugated sheets and columns and repair methods using a sensitivity analysis", *Eng. Failure Anal.*, **18**(8), 2064-2083. https://doi.org/10.1016/j.engfailanal.2011.06.013.

Lavassas I., Nikolaidis G., Zervas P., Efthimiou E., Doudoumis I.N., Baniotopoulos C.C. (2003), "Analysis and design of the prototype of a steel 1-MW wind turbine tower", *Eng. Struct.*, **25**(8), 1097–1106. https://doi.org/10.1016/S0141-0296(03)00059-2.

Lee, K.C. and Yoo, C.H. (2012), "Longitudinal Stiffeners in Concrete-Filled Tubes", *J. Struct. Eng.*, **138**(6), 753-758. https://doi.org/10.1061/(ASCE)ST.1943-541X.0000526.

Lemak, D. and Studnicka, J. (2005), "Influence of Ring Stiffeners on a Steel Cylindrical Shell", *Acta Polytechnica*, **45**(1), 56-63.

Lupi, F., Borri, C., Facchini, L., Niemann, H.J. and Peil, U. (2013), "A new type of bistable flow around circular cylinders with spanwise stiffening rings", *J. Wind Eng. Industrial Aerodynam.*, **123**(6), 281-290. https://doi.org/10.1016/j.jweia.2013.09.004.

Makarios, T. and Baniotopoulos, C.C. (2014), "Wind Energy Structures: Modal Analysis by the Continuous Model Approach", *J. Vib. Control.*, **20**(3), 395-405. https://doi.org/10.1177%2F1077546312463761.

Nguyen T.-C., Huynh T.-C., Kim J.-T. (2015), "Numerical evaluation for vibration-based damage detection in wind turbine tower structure", *Wind Struct.*, **21**(6), 657-675. http://dx.doi.org/10.12989/was.2015.21.6.657.

Nguyen T.-C., Huynh T.-C., Yi J.-H. and Kim J.-T. (2017), "Hybrid bolt-loosening detection in wind turbine tower structures by vibration and impedance responses", *Wind Struct.*, **24**(4), 385-403. https://doi.org/10.12989/was.2017.24.4.385.

Qu, Y., Wu, S., Chen, Y. and Hua, H. (2013), "Vibration analysis of ring-stiffened conical–cylindrical–spherical shells based on a modified variational approach", *J. Mech. Sci.*, **69**(4), 72-84. https://doi.org/10.1016/j.ijmecsci.2013.01.026.

Ramachandran, P. and Narayanan, S. (2007), "Evaluation of modal density, radiation efficiency and acoustic response of longitudinally stiffened cylindrical shell", *J. Sound Vib.*, **304**(1), 154-174. https://doi.org/10.1016/j.jsv.2007.02.020.

Rebelo C, Veljkovic M, Matos R, Simões da Silva L. (2012), "Structural monitoring of a wind turbine steel tower Part II monitoring results", *Wind Struct.*, **15**, 301-311.

Rebelo C, Veljkovic M, Simões da Silva L, Simões R, Henriques J. (2012), "Structural monitoring of a wind turbine steel tower Part I system description and calibration", *Wind Struct.*, **15**, 285-299. https://doi.org/10.12989/was.2012.15.4.285.

Ross, C.T.F., Little, A.P.F. and Adeniyi, K.A. (2005), "Plastic buckling of ring-stiffened conical shells under external

hydrostatic pressure", *Ocean Eng*., **32**(1), 21-36. https://doi.org/10.1016/j.oceaneng.2004.05.007.
Rotter, J.M. and Sadowski, A.J. (2012), "Cylindrical shell bending theory for orthotropic shells under general axisymmetric pressure distributions", *Eng. Struct.*, **42**(12), 258-265. https://doi.org/10.1016/j.engstruct.2012.04.024.
Sabouri-Ghomi, S., Kharrazi, M.H.K. and Javidan, P. (2006), "Effect of stiffening rings on buckling stability of R.C. hyperbolic cooling towers", *Thin-Wall. Struct.*, **44**(2), 152-158. https://doi.org/10.1016/j.tws.2006.02.005.
Showkati, H. and Shahandeh, R. (2010), "Experiments on the Buckling Behavior of Ring-Stiffened Pipelines under Hydrostatic Pressure", *J. Eng. Mech.*, **136**(4), 464-471. https://doi.org/10.1061/(ASCE)EM.1943-7889.0000080.
Torkamani, S., Navazi, H.M., Jafari, A.A. and Bagheri, M. (2009), "Structural similitude in free vibration of orthogonally stiffened cylindrical shells", *Thin-Wall. Struct.*, **47**(11), 1316-1330.
Wójcik, M., Iwicki, P. and Tejchman, J. (2011), "3D buckling analysis of a cylindrical metal bin composed of corrugated sheets strengthened by vertical stiffeners", *Thin-Wall. Struct.*, **49**(8), 947-963. https://doi.org/10.1016/j.tws.2011.03.010.
Xie, W. and Sun, L. (2009), "Structural Noise of Longitudinal Stiffened Concrete Cylindrical Shell", *ICCTP 2009: Critical Issues in Transportation Systems Planning, Development, and Management*, 3361-3367. Harbin, China, 5-9 August.
Zhao, X., Liew, K.M. and Ng, T.Y. (2002), "Vibrations of rotating cross-ply laminated circular cylindrical shells with stringer and ring stiffeners", *J. Solids Struct.*, **39**(2), 529-545. https://doi.org/10.1016/S0020-7683(01)00194-9.

PL